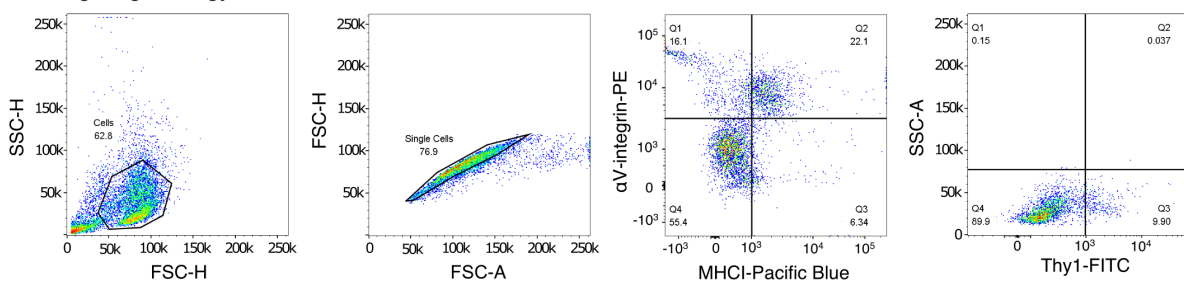


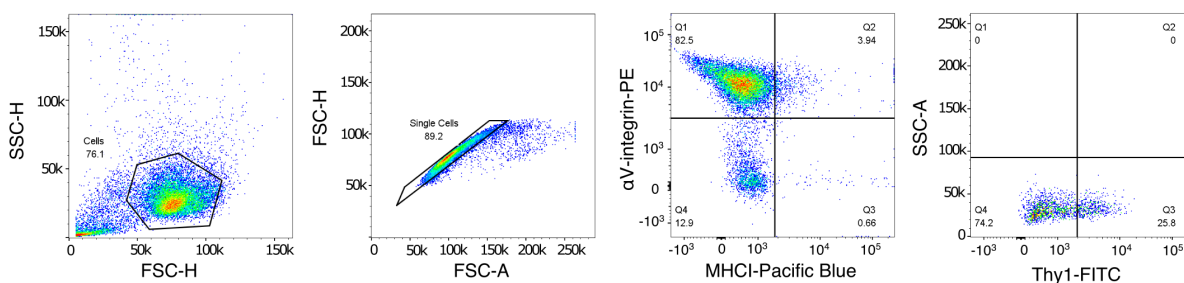
Figure S1

A

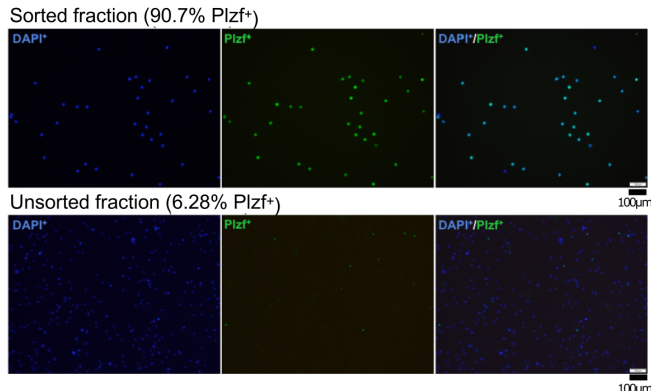
PND8 gating strategy



PND15 gating strategy



B



C

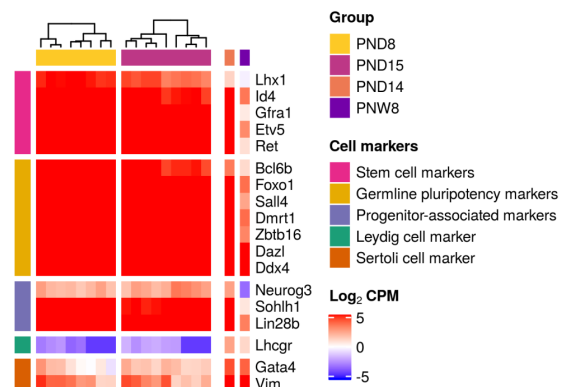


Figure S1. FACS of spermatogonial cells leads to high enrichment of PLZF⁺ cells

- (A) Representative dot plots of the sorting strategy for spermatogonial cell enrichment. Gating based on side scatter/forward scatter (SSC-A/FSC-A) and forward scatter – height/ forward scatter – area (FSC-H/FSC-A) was performed to exclude cell debris and cell clumps;
- (B) Immunocytochemistry cell samples before and after enrichment of spermatogonial cells. Immunocytochemistry of PND15 unsorted and sorted testis cell suspension was performed by fixating the cells on poly-L-lysine coated slides. Cells were stained with anti-PLZF antibody (S19 clone, Active Motif) and VECTASHIELD (with DAPI) antifade mounting medium was used for mounting. Cells were visualized under a fluorescence microscope and counted in 10 different fields of view / slide. The number of PLZF⁺ and PLZF⁻ cells from 10 different fields of view was averaged;
- (C) Heatmap of the expression profile of selected markers of spermatogonial and different testicular somatic cells extracted from the RNA-seq data on PND8, PND15 samples and on literature PND14 and PNW8 samples. Key genes for stem cell potential, stem and progenitor spermatogonia, and Leydig and Sertoli cells were chosen to assess the enrichment of spermatogonial cells in the sorted cell populations. Gene expression is represented in Log₂CPM (counts per million).

Figure S2

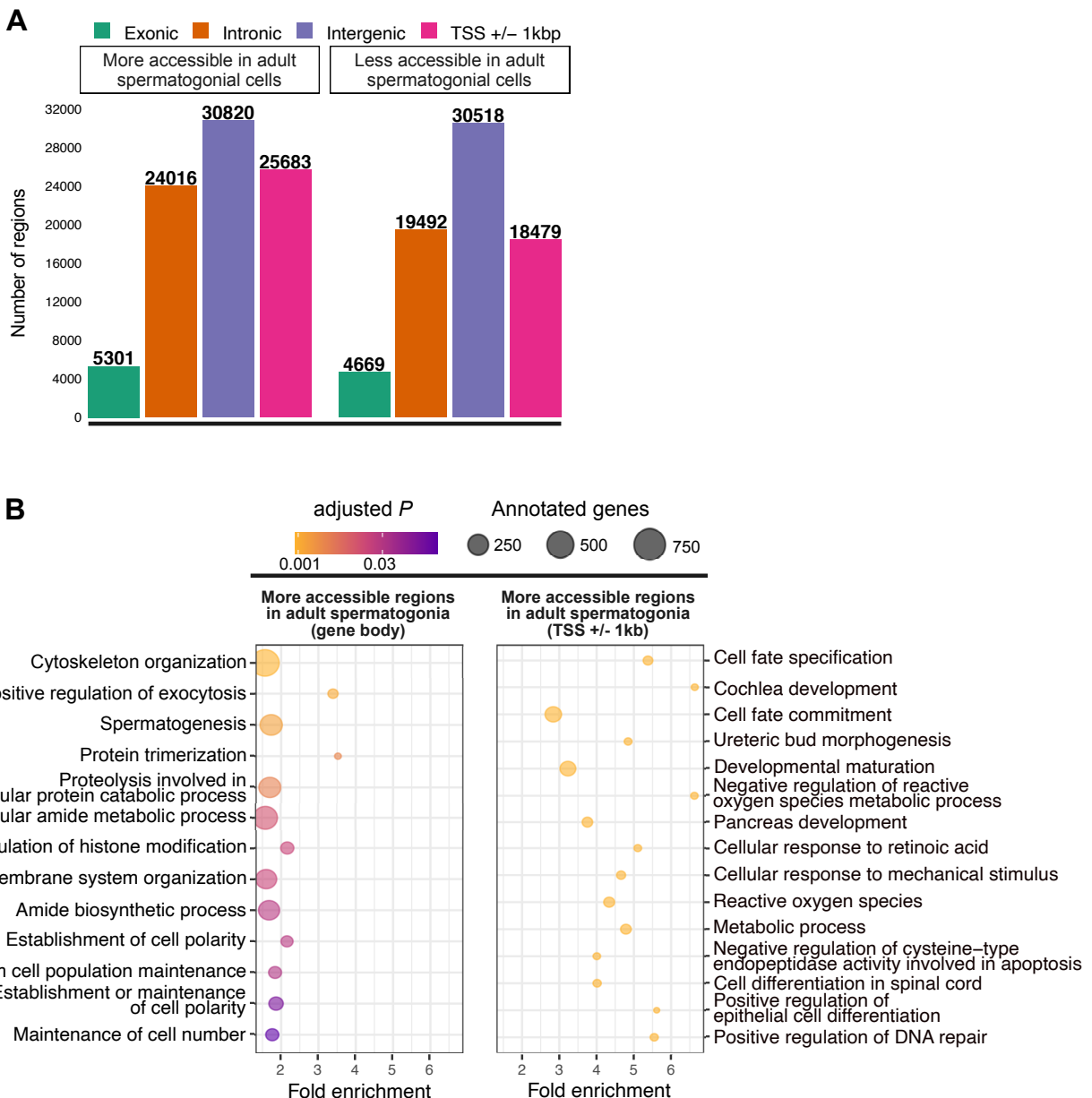


Figure S2. Omni-ATAC profiles of PND15 adult spermatogonial cell samples and their genomic distribution

- (A) Genomic distribution of the 158, 978 Omni-ATAC regions identified;
- (B) Dot plots of top enriched GO biological processes for regions with increased chromatin accessibility in adult spermatogonia, within gene bodies and around transcription starting sites (TSSs) of nearby genes (TSS +/- 1kb). The size of dots indicates the number of genes in the term and the color of each dot corresponds to the adjusted *P* value of the term's enrichment.

Figure S3

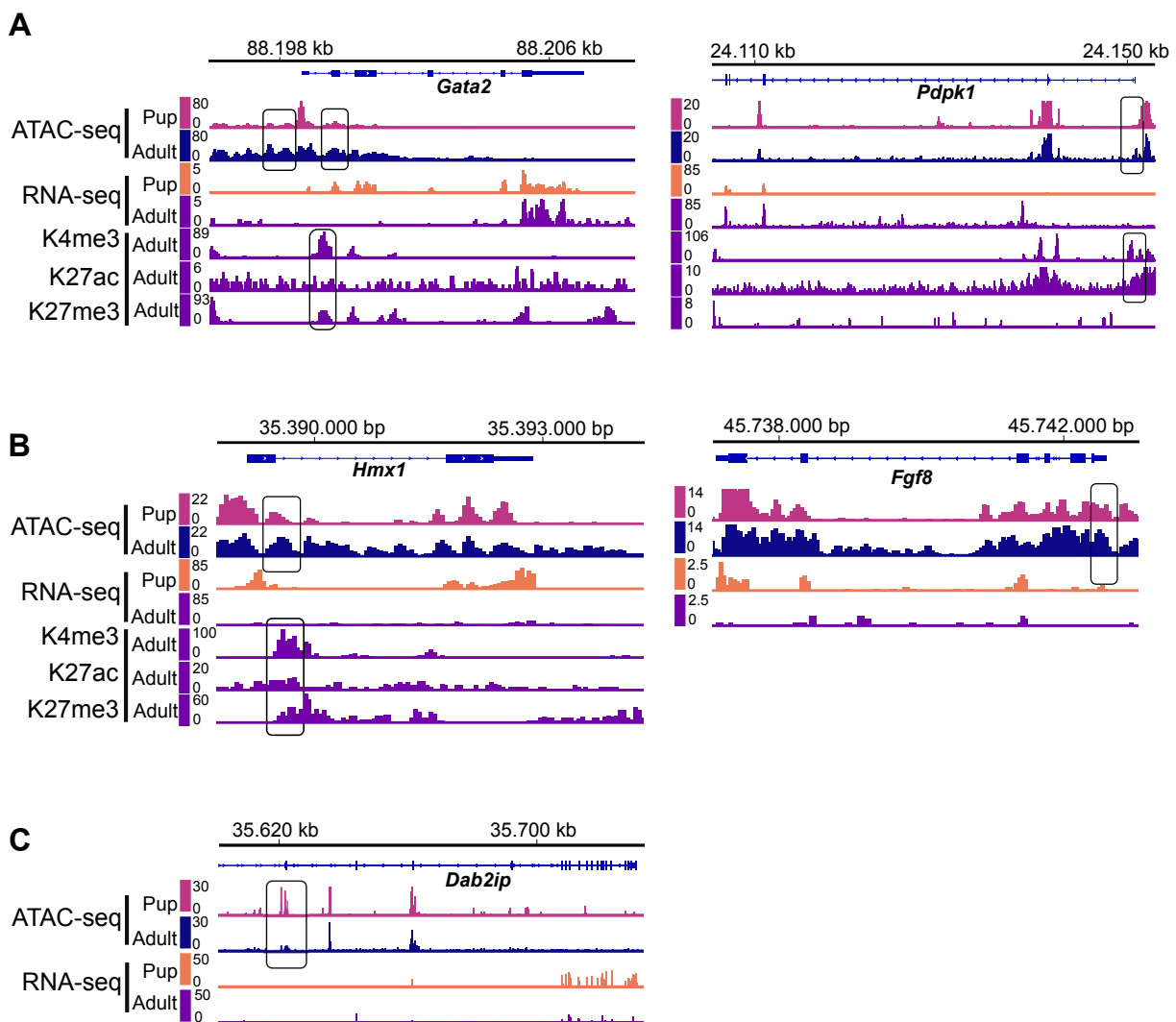


Figure S3. Representative examples from Categories 1-3 resulted from the overlap of chromatin accessibility, gene expression and histone profiling datasets

(A-C) Genomic snapshots from the Integrative Genomics Viewer (IGV, Broad Institute) of exemplary genes from Category 1 (*Gata2* and *Pdkp1*), Category 2 (*Hmx1* and *Fgf8*) and Category 3 (*Dab2ip*) showing relative abundance of: transcripts from RNA-seq, chromatin accessibility from ATAC-seq and enrichment of 3 different histone marks (H3K27ac, H3K4me3 and H3K27me3) from ChIP-seq. RNA-seq data corresponds to literature PND14 and adult (PNW8) spermatogonial cells and ATAC-seq data to PND15 and adult (PNW20) spermatogonial cells, respectively.

Figure S4

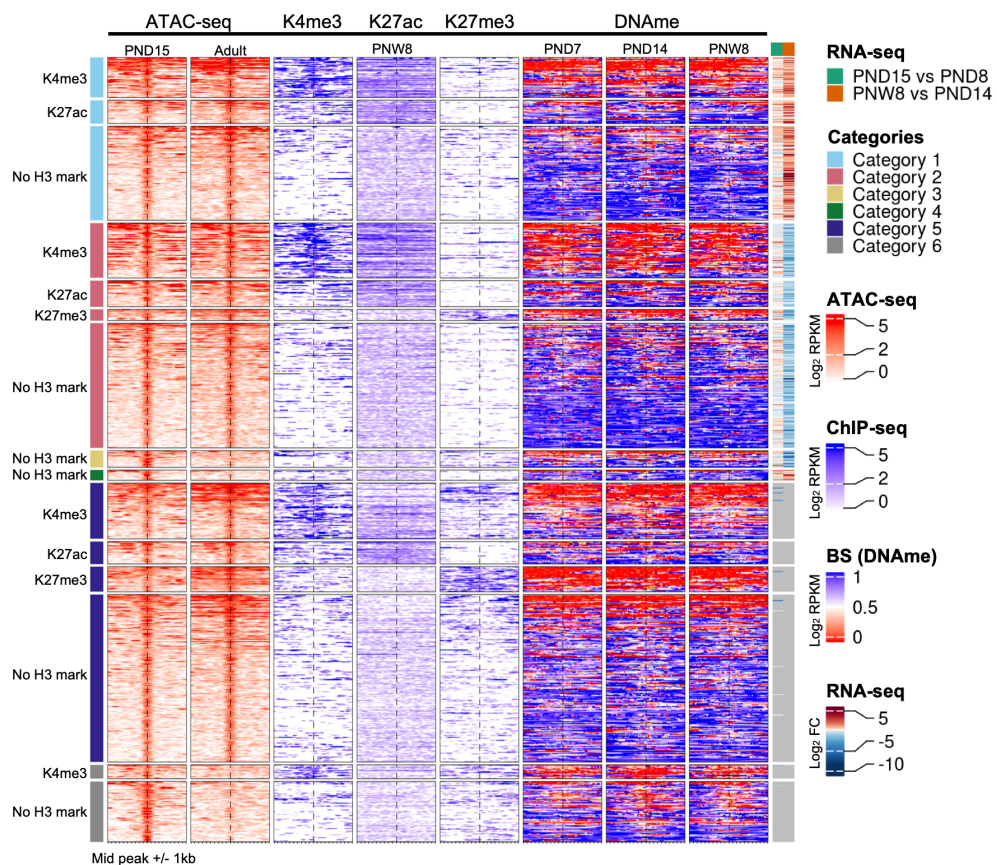


Figure S4. DNAme profiles of spermatogonial cells do not show major changes over the period of testis postnatal maturation

Enriched heatmaps showing the overlap between Category 1-4 regions, literature ChIP-seq data in PNW8 spermatogonia for H3K4me3, H3K27ac and H3K27me3, and DNAme data from BS in PND7, PND14 and PNW8 spermatogonia. For each of the Category 1-4 the following sub-categorization was applied:

- Regions that are enriched for H3K4me3 (with or w/o H3K27ac and/or H3K27me3)
- Regions that are enriched for H3K27ac (and lack both H3K4me3 and H3K27me3)
- Regions that are enriched for H3K27me3 (and lack both H3K4me3 and H3K27ac)

Each line represents a peak region and the regions are ordered by the ATAC-seq signal. Mid-x-axis corresponds to the middle of a peak region and is extended to +/- 1 kbp. The color-key of the ATAC-seq, ChIP-seq and BS heatmaps represent ATAC-seq, ChIP-seq and BS signal, respectively. For RNA-seq, log₂ FC is shown from PND8 vs PND15 and PND14 vs PNW8 comparisons. For BS, the level of DNAme is between 0 and 1, with 0 representing completely unmethylated loci and 1 fully methylated loci, respectively.

Figure S5

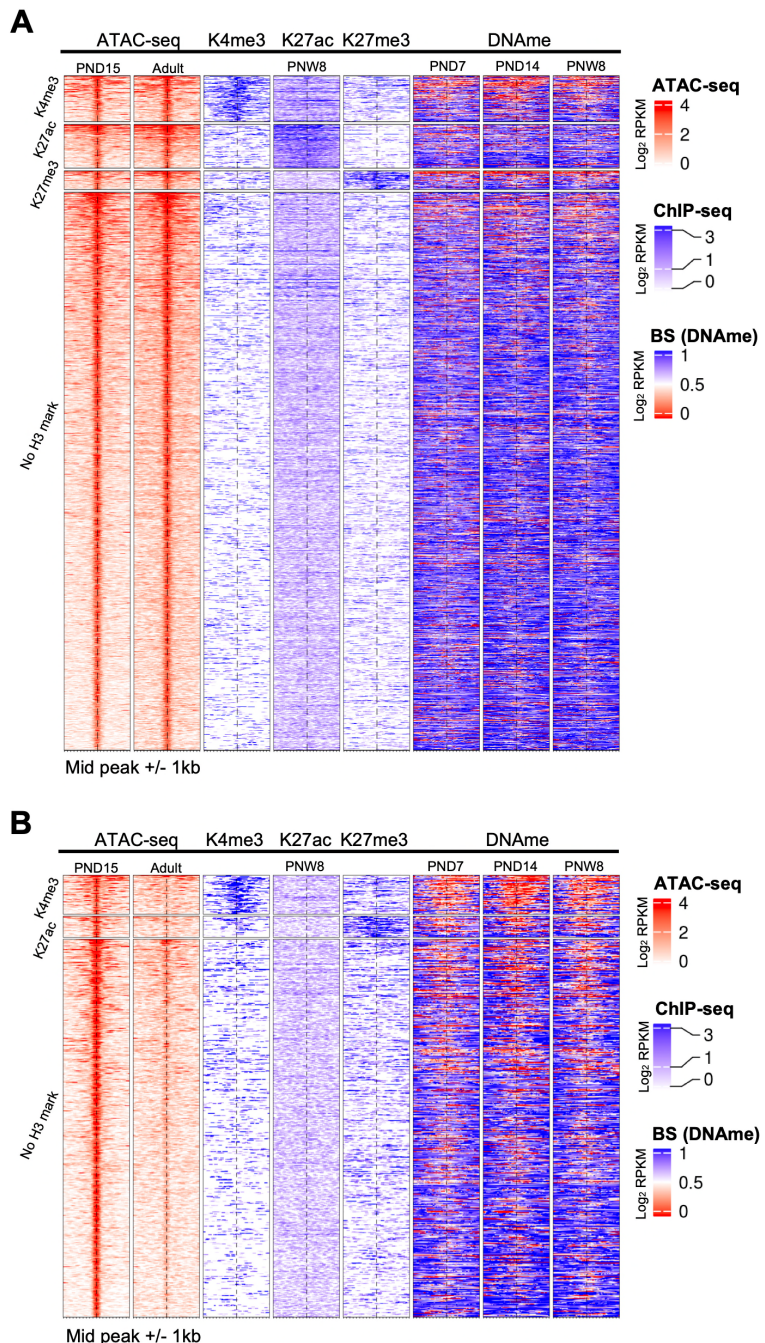


Figure S5. Distinct chromatin profiles between PND15 and adult spermatogonia are present at distal regions across the genome

(A-B) Enriched heatmaps showing the overlap between more accessible regions (A) and less accessible regions (B) situated in distal regions in spermatogonial cells, and literature ChIP-seq and DNAme data in PNW8 spermatogonia. The same categorisation as in Figure S4 was applied. Each line represents a peak region and the regions are ordered by the ATAC-seq signal. Mid-x-axis corresponds to the middle of a peak region and is extended to +/- 1 kbp. The color-key of the ATAC-seq, ChIP-seq and BS heatmaps represent ATAC-seq, ChIP-seq and BS signal, respectively. For BS, the level of DNAme is between 0 and 1, with 0 representing completely unmethylated loci and 1 fully methylated loci, respectively.

Figure S6

A

Enriched TF motifs in less accessible ERVKs in adult spermatogonia			Enriched TF motifs in less accessible LINE L1s in adult spermatogonia		
TF	Enriched motif	% of target sequences	TF	Enriched motif	% of target sequences
PBX3		24.15%	FO XO1		15.02%
THAP11		22.25%	ZEB1		14.7%
ZNF143		27.21%	E2F3		13.79%
FOXL1		24.53%	KLF5		12.67%
NF-YA		25.88%	ZBTB17		12.74%

B

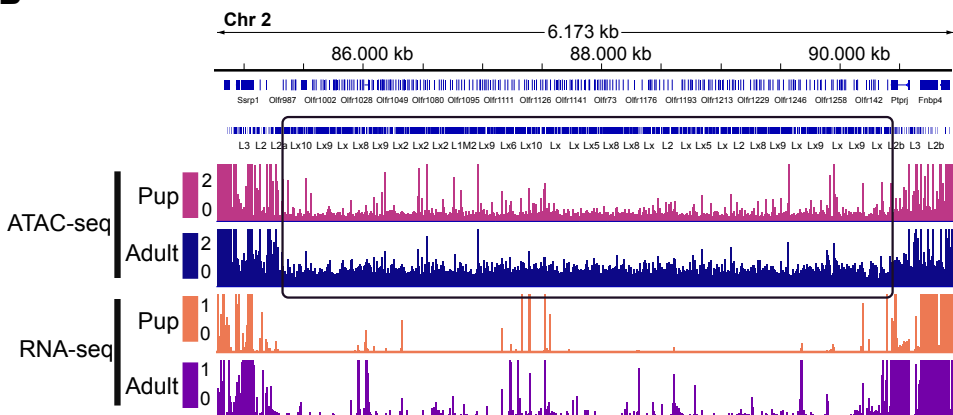


Figure S6. Differentially accessible TEs exhibit enriched TF motifs and correspond to regions nearby non-random gene families

- A. HOMER extracted consensus sequences for TF motifs enriched in less accessible ERVK subtypes and less accessible LINE L1 subtypes. Representative examples from the most enriched transcription factor families are depicted;
- B. Genomic snapshots from the Integrative Genomics Viewer (IGV, Broad Institute) of a cluster of *Olfr* genes on Chr2 with an increased density of LINE elements. The relative abundance of transcripts from RNA-seq and chromatin accessibility from ATAC-seq are shown. RNA-seq data corresponds to literature PND14 and adult (PNW8) spermatogonial cells and ATAC-seq data to PND15 and adult (PNW20) spermatogonial cells, respectively.